Article

# Organolanthanide-Mediated Intramolecular Hydroamination/Cyclization of Conjugated Aminodienes: A Computational Exploration of Diverse Mechanistic Pathways for the Regioselective Generation of Functionalized Azacycles Supported by a Lanthanocene-Based Catalyst Complex

Sven Tobisch

*J. Am. Chem. Soc.*, **2005**, 127 (34), 11979-11988• DOI: 10.1021/ja042546h • Publication Date (Web): 05 August 2005



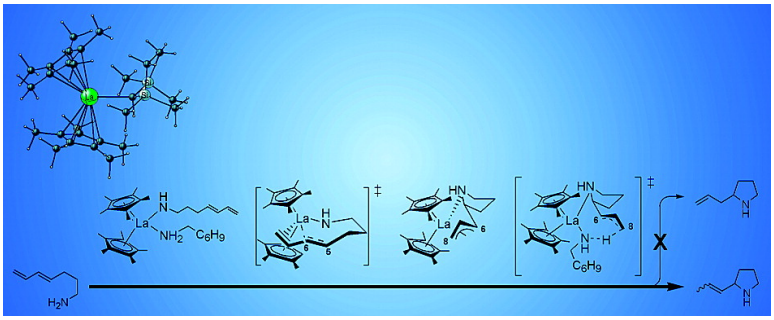

## More About This Article

Additional resources and features associated with this article are available within the HTML version:

- Supporting Information
- Links to the 9 articles that cite this article, as of the time of this article download
- Access to high resolution figures
- Links to articles and content related to this article
- Copyright permission to reproduce figures and/or text from this article

View the Full Text HTML

J|A|C|S
ARTICLES
Published on Web 08/05/2005

# Organolanthanide-Mediated Intramolecular Hydroamination/Cyclization of Conjugated Aminodienes: A Computational Exploration of Diverse Mechanistic Pathways for the Regioselective Generation of Functionalized Azacycles Supported by a Lanthanocene-Based Catalyst Complex

Sven Tobisch

*Contribution from the Institut für Anorganische Chemie der Martin-Luther-Universität Halle-Wittenberg, Fachbereich Chemie, Kurt-Mothes-Strasse 2, D-06120 Halle, Germany*

Received December 11, 2004; E-mail: tobisch@chemie.uni-halle.de

***Abstract:*** The complete catalytic reaction course for the organolanthanide-mediated intramolecular hydroamination/cyclization (IHC) of (4*E*,6)-heptadien-1-amine by a prototypical achiral $Cp^*_2LaCH(TMS)_2$ precatalyst is critically scrutinized by employing a gradient-corrected DFT method. The condensed free-energy profile for the overall reaction, comprised of thermodynamic and kinetic aspects of individual elementary steps, is presented. A computationally verified, revised mechanistic scenario has been proposed, which is consistent with the empirical rate law, accounts for crucial experimental observations, and provides a first understanding of the origin of the measured negative $\Delta S^{\ddagger}$. It involves rapid substrate association/dissociation equilibria and facile intramolecular diene insertion, linked to turnover-limiting protonolysis of the $\eta^3$-butenyl−Ln functionality, with the amine-amidodiene−Ln adduct complex representing the catalyst's resting state. The thermodynamic and kinetic factors that determine the high regio- and stereoselectivity of the mechanistically diverse IHC of aminodienes have been elucidated. These achievements allow a deeper understanding and a consistent rationalization of the experimental results for aminodiene IHC and furthermore enhance the insights into general mechanistic aspects of the organolanthanide-mediated cycloamination.

## Introduction

Catalytic carbon−nitrogen bond-forming processes are of utmost importance in synthetic organic chemistry. Hydroamination, viz. the catalytic addition of a N−H bond across unsaturated carbon−carbon functionalities, represents an efficient, atom-economical, and desirable route to nitrogen-containing molecules that are important for a variety of applications.[1] There has been a growing effort in the past to develop efficient and selective catalysts for this highly valuable but challenging transformation covering various C−C unsaturations that are mediated by early[2] and late[3] transition metals, as well as by rare earth elements.[4]

Organolanthanide complexes[5,6] have received particular attention because they exhibit different reactivity from transition-metal d-element congeners. This distinct behavior originates from (i) the highly electrophilic, kinetically labile f-element centers, which are compatible with a variety of nondissociable ancillary ligands, (ii) a generally single, thermodynamically stable oxidation state ($Ln^{3+}$), which gives rise to the absence of conventional oxidative-addition/reductive-elimination processes, (iii) the relatively large ionic radii together with large possible coordination numbers, and (iv) corelike $4f^n$ orbitals, which renders the chemistry of lanthanides highly ionic, thus governing the lanthanide−ligand interaction mainly by electrostatic and steric factors, rather than by orbital interaction forces.

Organolanthanides have been shown to catalyze the hydroamination of alkene, alkyne, allene, and 1,3-diene functionalities

(1) For reviews of catalytic hydroamination, see: (a) Hegedus, L. S. *Angew. Chem., Int. Ed. Engl.* **1988**, *27*, 1113. (b) Roundhill, D. M. *Catal. Today* **1997**, *37*, 155. (c) Müller, T. E.; Beller, M. *Chem. Rev.* **1988**, *88*, 675. (d) Brunet, J. J.; Neibecker, D. In *Catalytic Heterofunctionalization*; Togni, A., Grützmacher, H., Eds.; Wiley-VCH: Weinheim, 2001; pp 91−141. (e) Nobis, M.; Driessen-Hölscher, B. *Angew. Chem., Int. Ed.* **2001**, *40*, 3983. (f) Taube, R. In *Applied Homogeneous Catalysis with Organometallic Complexes*; Cornils, B., Herrmann, W. A., Eds.; Wiley-VCH: Weinheim, Germany, 2002; pp 513−524. (g) Pohlki, F.; Doye, S. *Chem. Soc. Rev.* **2003**, *32*, 104.

(2) For hydroamination mediated by early transition metals, see: (a) Pohlki, F.; Doye, S. *Angew. Chem., Int. Ed.* **2001**, *40*, 2305. (b) Johnson, J. S.; Bergmann, R. G. *J. Am. Chem. Soc.* **2001**, *123*, 2923. (c) Cao, C.; Ciszewski, J. T.; Odom, A. L. *Organometallics* **2001**, *20*, 5011. (d) Straub, B. F.; Bergman, R. G. *Angew. Chem., Int. Ed.* **2001**, *40*, 4632. (e) Ackermann, L.; Bergmann, R. G. *Org. Lett.* **2002**, *4*, 1475. (f) Ong, T.-G.; Yap, G. P. A.; Richeson, D. S. *Organometallics* **2002**, *21*, 2839. (g) Tillack, A.; Castro, I. G.; Hartung, C. G.; Beller, M. *Angew. Chem., Int. Ed.* **2002**, *41*, 2541. (h) Shi, Y.; Hall, C.; Ciszewski, J. T.; Cao, C.; Odom, A. L. *Chem. Commun.* **2003**, 586.

(3) For hydroamination mediated by late transition metals, see: (a) Müller, T. E.; Grosche, M.; Herdtweck, E.; Pleier, A.-K.; Walter, E.; Yan, Y.-K. *Organometallics* **2000**, *19*, 170. (b) Vasen, D.; Salzer, A.; Gerhards, F.; Gais, H.-J.; Stürmer, R.; Bieler, N. H.; Togni, A. *Organometallics* **2000**, *19*, 539. (c) Kawatsura, M.; Hartwig, J. F. *Organometallics* **2001**, *20*, 1960. (d) Müller, T. E.; Berger, M.; Grosche, M.; Herdtweck, E.; Schmidtchen, F. P. *Organometallics* **2001**, *20*, 4384. (e) Hartung, C. G.; Tillack, A.; Trauthwein, H.; Beller, M. *J. Org. Chem.* **2001**, *66*, 6339. (f) Nettekoven, U.; Hartwig, J. F. *J. Am. Chem. Soc.* **2002**, *124*, 1166. (g) Neff, V.; Müller, T. E.; Lecher, J. A. *Chem. Commun.* **2002**, 906. (h) Fadini, L.; Togni, A. *Chem. Commun.* **2003**, 30.

in a highly regioselective and stereoselective fashion. Marks and co-workers have pioneered the intramolecular hydroamination/cyclization (IHC) of amine-tethered C−C unsaturations.[7] As an example, the transformation of primary and secondary amines tethered to conjugated dienes into five-, six-, and seven-membered azacycles bearing α-side chains proceeds in very high regioselectivity and good stereoselectivity, thereby offering an elegant, concise route toward the construction of naturally occurring alkaloid skeletons.[7,8] The organolanthanide-supported 1,3-diene hydroamination has been extended by Marks and co-workers to an intermolecular version,[9] while the intermolecular 1,3-diene hydroamination by late transition metal complexes has been advanced by the groups of Hartwig[10] and Ozawa.[11]

The comprehensive kinetic and mechanistic studies by Marks et al. led to a generally accepted mechanistic scenario for organolanthanide-supported IHC that bears features common to the various unsaturated C−C functionalities.[7] After smooth precatalyst activation, a large negative activation entropy was measured and the reaction rate is zero-order in [amine substrate] and first-order in [catalyst]. These observations led Marks to suggest a highly organized transition-state structure for the turnover-limiting step, which he proposed to be intramolecular cyclization for each of the various C−C unsaturations.

Despite the fact that these experimental investigations provided the first detailed insight into the IHC process, there are some crucial aspects that need to be elucidated further. These consist of, for instance, the identity of the turnover-limiting step, the origin of the large negative value of $\Delta S^{\ddagger}$, and the particularly important question about what factors govern the observed high regio- and stereoselectivity. In this regard a thorough computational examination can complement experiments by revealing information that is not available from experimental methods. Unfortunately, only a single computational study dealing with aminoalkene IHC has been reported thus far.[12a] This study predicted intramolecular cyclization to be rate-determining and protonolysis of the alkyl−Ln functionality of the azacyclic intermediate to be only slightly favored kinetically over C═C insertion into the Ln−N bond ($\Delta\Delta G^{\ddagger} = 1.2$ kcal mol$^{-1}$). The computational investigation did not address whether the additional substrate in the catalytic system[4b,7,8] can facilitate any of the individual elementary steps. This aspect, however, is of crucial importance for revealing a realistic mechanistic picture. Furthermore, the reported activation enthalpy and entropy for the turnover-limiting cyclization were determined with respect to an amidoalkene−Ln species,[12b] instead of relative to the catalyst's resting state, which is an amine-amidodiene−Ln adduct complex.[4b,7,8] Therefore, the computed energy profile cannot be compared directly with the experimentally derived kinetics for aminoalkene IHC.[4b]

Herein we present, to the best of our knowledge, the first comprehensive computational investigation of the salient mechanistic features of the organolanthanide-mediated IHC of conjugated aminodienes that covers the complete sequence of crucial elementary steps. The aim of this study is 2-fold: first, to explore general mechanistic aspects of the cycloamination, viz. catalyst formation, reaction kinetics, turnover-limiting step, for the aminodiene cycloamination taken as an example, and second, to unravel the key catalytic question about what the thermodynamic and kinetic factors are that control the selectivity. With respect to the second issue we decided to explore the IHC of aminodienes, which is likely to be mechanistically most diverse among the various C−C unsaturations (Scheme 1). In this regard, the observed high selectivity is even more remarkable, when, for instance, compared with cycloamination of aminoalkenes. The following intriguing aspects will be explored: (1) What are the crucial structural and energetic features of the individual elementary steps? (2) Which of the various steps is likely to be assisted by excess aminodiene substrate? (3) Which step is turnover-limiting? (4) What is the origin of the large negative $\Delta S^{\ddagger}$? (5) Which factors determine the regioselectivity of the cyclization and protonolysis steps? (6) What governs the stereoselectivity?

(4) For hydroamination mediated by rare earth metals, see: (a) Gagné, M. R.; Marks, T. J. *J. Am. Chem. Soc.* **1989**, *111*, 4108. (b) Gagné, M. R.; Stern, C. L.; Marks, T. J. *J. Am. Chem. Soc.* **1992**, *114*, 275. (c) Li, Y.; Marks, T. J. *J. Am. Chem. Soc.* **1996**, *118*, 9295. (d) Molander, G. A.; Dowdy, E. D. *J. Org. Chem.* **1998**, *63*, 8983. (e) Li, Y.; Marks, T. J. *J. Am. Chem. Soc.* **1998**, *120*, 1757. (f) Arredondo, V. M.; McDonald, F. E.; Marks, T. J. *Organometallics* **1999**, *18*, 1949. (g) Arredondo, V. M.; Tian, S.; McDonalds, F. E.; Marks, T. J. *J. Am. Chem. Soc.* **1999**, *121*, 3633. (h) Kim, Y. K.; Livinghouse, T.; Bercaw, J. E. *Tetrahedron Lett.* **2001**, *42*, 2933. (i) Kim, Y. K.; Livinghouse, T. *Angew. Chem., Int. Ed.* **2002**, *41*, 3645. (j) Wang, J.; Dash, A. K.; Kapon, M.; Berthet, J.-C.; Ephritikhine, M.; Eisen, M. S. *Chem. Eur. J.* **2002**, *8*, 5384. (k) Kim, Y. K.; Livinghouse, T.; Horino, Y. *J. Am. Chem. Soc.* **2003**, *125*, 9560. (l) Gribkov, D. V.; Hultzsch, K. C.; Hampel, F. *Chem. Eur. J.* **2003**, *9*, 4796. (m) Stubbert, B. D.; Stern, C. L.; Marks, T. J. *Organometallics* **2003**, *22*, 4836. (n) Ryu, J.-S.; Marks, T. J.; McDonald, F. E. *J. Org. Chem.* **2004**, *69*, 1038.

(5) For organolanthanide reviews, see: (a) Marks, T. J.; Ernst, R. D. In *Comprehensive Organometallic Chemistry*; Wilkinson, G., Stone, F. G. A., Abel, E. W., Eds.; Pergamon Press: Oxford, U.K., 1982; Chapter 21. (b) Evans, W. J. *Adv. Organomet. Chem.* **1985**, *24*, 131. (c) Schaverien, C. J. *Adv. Organomet. Chem.* **1994**, *36*, 283. (d) Schumann, H.; Meese-Marktscheffel, J. A.; Esser, L. *Chem. Rev.* **1995**, *95*, 865. (e) Edelmann, F. T. In *Comprehensive Organometallic Chemistry*; Wilkinson, G., Stone, F. G. A., Abel, E. W., Eds.; Pergamon Press: Oxford, U.K., 1995; Vol. 4, Chapter 2. (f) Bochkarev, M. N. *Chem. Rev.* **2002**, *102*, 2089. (g) Arndt, S.; Okuda, J. *Chem. Rev.* **2002**, *102*, 1953. (h) Edelmann, F. T.; Freckmann, D. M. M.; Schumann, H. *Chem. Rev.* **2002**, *102*, 1851. (i) Aspinall, H. C. *Chem. Rev.* **2002**, *102*, 1807.

(6) For reviews on organolanthanide catalysis, see: (a) Jeske, G.; Lauke, H.; Mauermann, H.; Schumann, H.; Marks, T. J. *J. Am. Chem. Soc.* **1985**, *107*, 8111. (b) Watson, P. L.; Parshall, G. W. *Acc. Chem. Res.* **1985**, *18*, 51. (c) Heeres, H. J.; Renkema, J.; Booji, M.; Meetsma, A.; Teuben, J. H. *Organometallics* **1988**, *7*, 2495. (d) Molander, G. A.; Hoberg, J. O. *J. Org. Chem.* **1992**, *57*, 3266. (e) Shapiro, P. J.; Cotter, W. D.; Schaefer, W. P.; Labinger, J. A.; Bercaw, J. E. *J. Am. Chem. Soc.* **1994**, *116*, 4623. (f) Fu, P.-F.; Brard, L.; Li, Y.; Marks, T. J. *J. Am. Chem. Soc.* **1995**, *117*, 7157. (g) Edelmann, F. T. *Top. Curr. Chem.* **1996**, *179*, 247. (h) Molander, G. A. *Chemtracts: Org. Chem.* **1988**, *18*, 237. (i) *Topics in Organometallic Chemistry*; Kobayashi, S., Ed.; Springer: Berlin, Germany, 1999; Vol. 2. (j) Hou, Z.; Wakatsuki, Y. *Coord. Chem. Rev.* **2002**, *231*, 1. (k) Molander, G. A.; Romero, J. A. C. *Chem. Rev.* **2002**, *102*, 2161. (l) Shibasaki, M.; Yoshikawa, N. *Chem. Rev.* **2002**, *102*, 2187. (m) Inanaga, J.; Furuno, H.; Hayano, T. *Chem. Rev.* **2002**, *102*, 2211.

(7) Hong, S.; Marks, T. J. *Acc. Chem. Res.* **2004**, *37*, 673.

(8) (a) Hong, S.; Marks, T. J. *J. Am. Chem. Soc.* **2002**, *124*, 7886. (b) Hong, S.; Kawaoka, A. M.; Marks, T. J. *J. Am. Chem. Soc.* **2003**, *125*, 15878. (c) Hong, S.; Tian, S.; Metz, M. V.; Marks, T. J. *J. Am. Chem. Soc.* **2003**, *125*, 14768. (d) Typical reaction conditions for the regioselective organolanthanide-mediated intramolecular hydroamination/cyclization (IHC) of aminodienes are: 40−80-fold molar excess of the substrate (for example, (4*E*,6)-heptadien-1-amine) together with the precatalyst (for example, $Cp^*_2LaCH(TMS)_2$) at 25 °C in noncoordinating solvents, viz. benzene, toluene, pentane, and cyclohexane. The following kinetics were experimentally determined for the IHC of (4*E*,6)-heptadien-1-amine mediated by the $Cp^*_2LaCH(TMS)_2$ precatalyst that affords a 84:16 mixture of *E*/*Z*-isomers of 2-(prop-1-enyl)pyrrolidine exclusively: $\Delta H^{\ddagger} = 10.4$ kcal mol$^{-1}$ and $\Delta S^{\ddagger} = -32.7$ eu; ref 8b)

(9) (a) Li, Y.; Marks, T. J. *Organometallics* **1996**, *15*, 3770. (b) Ryu, J.-S.; Li, G. Y.; Marks, T. J. *J. Am. Chem. Soc.* **2003**, *125*, 12584.

(10) (a) Kawatsura, M.; Hartwig, J. F. *J. Am. Chem. Soc.* **2000**, *122*, 9546. (b) Löber, O.; Kawatsura, M.; Hartwig, J. F. *J. Am. Chem. Soc.* **2001**, *123*, 4366. (c) Pawlas, J.; Nakao, Y.; Kawatsura, M.; Hartwig, J. F. *J. Am. Chem. Soc.* **2002**, *124*, 3669.

(11) Minami, T.; Okamoto, H.; Ikeda, S.; Tanaka, R.; Ozawa, F.; Yoshifuji, M. *Angew. Chem., Int. Ed.* **2001**, *40*, 4501.

(12) (a) Motta, A.; Lanza, G.; Fragala, I. L.; Marks, T. J. *Organometallics* **2004**, *23*, 4097. (b) It should be noted that this amidoalkene−Ln species with a nonchelating amidoalkene functionality is not the prevalent form of the amine-free amidoalkene−Ln complex (ref 12a). The reported values of $\Delta H^{\ddagger} = 7.7$ kcal mol$^{-1}$ and $\Delta S^{\ddagger} = -14.6$ eu for intramolecular cyclization, therefore, do not relate to the intrinsic kinetics for this step either.

***Scheme 1.*** General Catalytic Reaction Course for the Organolanthanide-Mediated Intramolecular Hydroamination/Cyclization of Aminodienes[a,b]

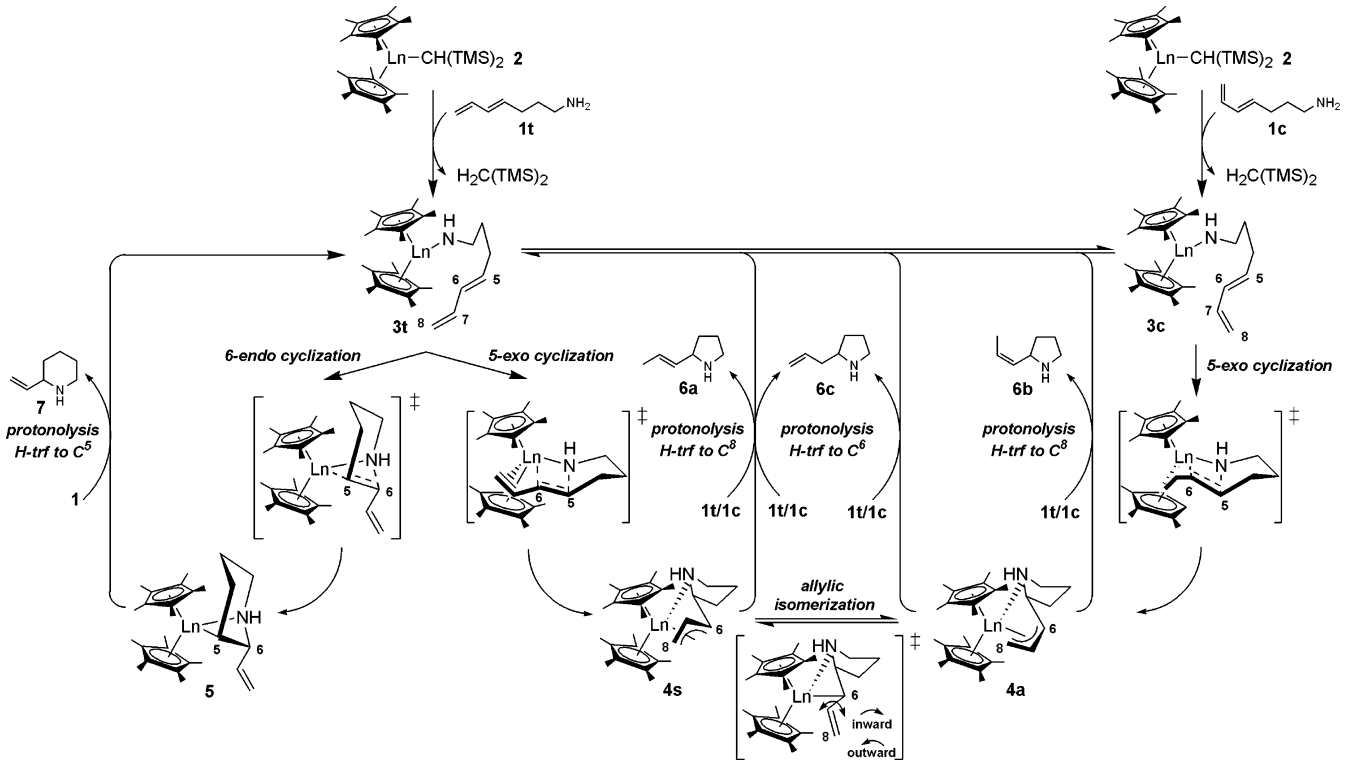


[a] Based on experimental studies of Marks and co-workers.[7,8] [b] The (4*E*,6)-heptadien-1-amine **1t** and the $Cp^*_2LnCH(TMS)_2$ complex **2** were chosen as prototypical aminodiene substrate and precatalyst. Please note that for **3c** → **4a** cyclization the 6-*endo* pathway is omitted for the sake of clarity.

The elucidation of these aspects leads us to propose a computationally verified mechanistic scenario that accounts for crucial experimental observations and that is consistent with the derived empirical rate law. The detailed mechanistic insight presented herein should assist in the rational design of new catalysts and contribute to a deeper understanding of the catalytic structure−reactivity relationships.

**Proposed Catalytic Reaction Course.** Organolanthanide complexes of the general type $Cp^*_2LnCH(TMS)_2$ ($Cp^* = \eta^5$-$Me_5C_5$; Ln = La, Sm, Y; TMS = $SiMe_3$) have been reported, among others, to serve as effective precatalysts for the intramolecular hydroamination/cyclization of aminodienes.[8] Scheme 1 displays a general catalytic cycle for the organolanthanide-mediated IHC of aminodiene **1** by the $Cp^*_2LnCH(TMS)_2$ starting material **2**. Precatalyst **2** becomes activated via protonolysis by substrate **1** to liberate the $CH_2(TMS)_2$ hydrocarbyl ligand and generate the catalytically active amidodiene−Ln complex **3**, as trans (**3t**) and cis (**3c**) forms of the diene fragment. Compound **3** then undergoes insertion of the C═C bond of the diene moiety into the Ln−N functionality to afford azacyclic intermediates. With regard to the regiochemistry, this step can proceed through 5-*exo* and 6-*endo* cyclization, leading to the regioisomeric products **4** and **5** bearing a 2-substituted five-membered azacycle tethered to an allylic functionality or a 2-substituted six-membered azacycle with a vinylic α-side chain, respectively. As far as the butenyl−Ln coordination is concerned,[6g,6i,13,14] **4** can exist as isomers **4s** and **4a** with a syn-$\eta^3$ and an anti-$\eta^3$-butenyl−Ln bond, respectively, which are interconnected by allylic isomerization. The ensuing protonolysis of the azacyclic insertion products by **1** liberates the cycloamine products and regenerates the catalytically active compound **3**, thereby completing the catalytic cycle. Protonolysis of **5** yields the 2-vinyl-piperidine **7** along the 6-*endo* cyclization initiated route, while 2-propenyl-pyrrolidines **6a**−**6c** are the products of the alternative route that starts with 5-*exo* cyclization. Two regioisomeric pathways for protonolysis of **4s**, **4a** are distinguished by proton transfer to either of the two reactive allylic carbons. Proton transfer to the substituted $C^6$ center affords 2-(prop-2-enyl)pyrrolidine **6c**, while protonation of the unsubstituted terminal $C^8$ center gives rise to *E*- and *Z*-isomers of 2-(prop-1-enyl)pyrrolidine **6a**, **6b**, when starting from **4s** and **4a**, respectively.

The cycloamination of (4*E*,6)-heptadien-1-amine (**1t**) with $Cp^*_2LaCH(TMS)_2$ is a rapid process and occurs with high regioselectivity.[8a,b,d] Thus, 2-substituted pyrrolidines are exclusively formed with a good *E* double bond selectivity, as indicated by the observed product ratio of 84 (**6a**):16 (**6b**):0 (**6c**), while there is no evidence for the alternative 6-*endo*

(13) There is substantial precedent for $\eta^3$-allylic structures in organo-f-element chemistry; see: (a) Jeske, G.; Lauke, H.; Mauermann, H.; Swepston, P. N.; Schumann, H.; Marks, T. J. *J. Am. Chem. Soc.* **1985**, *107*, 8091. (b) Bunel, E.; Burger, B. J.; Bercaw, J. E. *J. Am. Chem. Soc.* **1988**, *110*, 976. (c) Nolan, S. P.; Stern, D.; Marks, T. J. *J. Am. Chem. Soc.* **1989**, *111*, 7844. (d) Evans, W. J.; Ulibarri, T. A.; Ziller, J. W. *J. Am. Chem. Soc.* **1990**, *112*, 2314. (e) Scholz, A.; Smola, A.; Scholz, J.; Löbel, J.; Schimann, H.; Thiele, K.-H. *Angew. Chem., Int. Ed. Engl.* **1991**, *30*, 435. (f) Evans, W. J.; Keyer, R. A.; Rabe, G. W.; Drummond, D. K.; Ziller, J. W. *Organometallics* **1993**, *12*, 4664. (g) Evans, W. J.; Gonzales, S. L.; Ziller, J. W. *J. Am. Chem. Soc.* **1994**, *116*, 2600.

(14) (a) Taube, R.; Windisch, H.; Görlitz, F.; Schumann, H. *J. Organomet. Chem.* **1993**, *445*, 85. (b) Taube, R.; Windisch, H. *J. Organomet. Chem.* **1994**, *472*, 71. (c) Taube, R.; Maiwald, St.; Sieler, J. *J. Organomet. Chem.* **1996**, *513*, 37. (d) Taube, R.; Windisch, H.; Maiwald, St.; Hemling, H.; Schumann, H. *J. Organomet. Chem.* **1996**, *513*, 49. (e) Taube, R.; Windisch, H.; Weissenborn, H.; Hemling, H.; Schumann, H. *J. Organomet. Chem.* **1997**, *548*, 229. (f) Taube, R.; Windisch, H.; Hemling, H.; Schumann, H. *J. Organomet. Chem.* **1998**, *555*, 201. (g) Taube, R.; Maiwald, St.; Sieler, J. *J. Organomet. Chem.* **2001**, *621*, 327.

cyclization. Experiments showed that the reaction rate is zero-order in [aminodiene substrate] and first-order in [catalyst] under the actual reaction conditions,[8] as expressed in the empirical law (eq 1),

$$\text{velocity} = k[\text{substrate}]^0[\text{Ln}]^1 \quad (1)$$

and that the process occurs with a large negative activation entropy ($\Delta S^{\ddagger} = -32.7$ eu).[8b] This $\Delta S^{\ddagger}$ is similar in magnitude to that reported for the intermolecular version of the process.[9]

## Computational Model and Method

**Model.** Herein we report the computational exploration of the cycloamination of (4*E*,6)-heptadien-1-amine **1t** by the real $Cp^*_2LaCH(TMS)_2$ precatalyst **2**. The studies include scrutinization of alternative pathways for each of the critical steps of the tentative catalytic cycle shown in Scheme 1.

**Method.** All calculations have been performed with the program package TURBOMOLE[15] using the BP86 density functional,[16] which has already been applied successfully to the description of both energetic and structural aspects of organolanthanide compounds.[17] The appropriateness of the BP86 functional for the reliable determination of the energy profile for the organolanthanide-supported IHC of aminodienes (cf. Supporting Information) and ring-opening polymerization of methylenecycloalkanes[18] has been demonstrated. Further details, together with a description of the employed computational methodology, are given in the Supporting Information. All the drawings were carried out by using the StrukEd program.[19]

## Results and Discussion

The theoretical exploration of the aminodiene cycloamination starts with the careful step-by-step exploration of the elementary steps outlined in Scheme 1. To elucidate the regulation of the selectivity, the various pathways conceivable for each of these steps have been scrutinized. The presentation of this first part of our study, however, is restricted to the favorable pathway that is traversed in the catalytic process; a complete account of the evaluation of each pathway is provided in the Supporting Information. In the second part, the condensed free-energy profile of the critical steps is presented, and general mechanistic aspects of the cycloamination process are elucidated. A further section is devoted to the control of regio- and stereoselectivity.

**I. Exploration of Crucial Elementary Steps. A. Precatalyst Activation.** To enter the catalytic cycle, the $Cp^*_2LaCH(TMS)_2$ starting material **2** first undergoes protonolysis by **1** to generate the amidodiene−La active catalyst complex by expulsion of $CH_2(TMS)_2$. Two alternative paths are conceivable that involve the thermodynamically favorable 4*E*(trans), **1t**, and the 4*Z*(cis), **1c**, substrate forms, respectively, thereby affording isomers **3t**, **3c** of the amidodiene−La complex having a transoid and cisoid diene tether functionality. Both paths exhibit almost identical structural features; for a detailed discussion, the reader is referred to the Supporting Information.

Protonolysis of **2** proceeds first with the formation of the substrate encounter complex **2**-S(t),[20] which is exothermic ($\Delta H = -5.2$ kcal mol$^{-1}$), but is endergonic with respect to the separated {**1t** + **2**} fragments ($\Delta G = 3.4$ kcal mol$^{-1}$). The barrier for subsequent proton transfer is moderate ($\Delta G^{\ddagger} = 14.3$ kcal mol$^{-1}$) and is connected with a small negative activation entropy of −2.4 eu (Table S1). The computed activation barrier is in good agreement with the observed turnover frequency for the precatalyst activation step,[4b,21] thereby indicating the suitability of the employed computational method for the reliable prediction of the energy profile. The catalytically active compound **3t** can exist in several forms. The initially formed protonolysis product species **3t′** with an $\eta^1$-amidodiene moiety readily transforms into species **3t″** that contains a chairlike chelating amidodiene moiety (Figure S1). Isomers **3t′**, **3t″** are predicted to be almost identical in free energy. The overall **1t** + **2** → **3t′**/**3t″** + $CH_2(TMS)_2$ transformation is exergonic by −22.9 kcal mol$^{-1}$ (Table S1). This implies (under the assumption that formation of possible side products is not effective) that the precatalyst is converted in an almost quantitative fashion into the catalytically active amidodiene−La complex in a first protonolysis step that is kinetically feasible. Compounds **3t′**, **3t″** complex aminodiene substrate, which is always present in excess.[8d] Substrate uptake in **3t″** comes at the expense of the diene−La interaction, such that **3t′**-S(t) with a noncoordinating $\eta^1$-amidodiene moiety becomes the prevalent adduct species (Figure S1). This kinetically facile association process[22] is exothermic ($\Delta H = -10.1$ kcal mol$^{-1}$), while the driving force becomes reduced to −2.4 kcal mol$^{-1}$ ($\Delta G$, Table 1) by taking the entropic penalty into account. Accordingly, complex **3** is predominantly present as substrate adduct **3t′**-S(t)[20] under catalytic reaction conditions (cf. section II.A).[8d,23]

**B. Intramolecular Cyclization.** Having the amidodiene−La catalyst complex **3** formed in a first smooth protonolysis step, intramolecular cyclization to afford azacyclic−La intermediates **4** or **5** is encountered next in the reaction course (Scheme 1). The discussion is primarily focused on the 5-*exo* pathway, its key species shown in Figure 1, while the 6-*endo* pathway is tackled only briefly (see the Supporting Information for more details). The complete energetics is compiled in Table 1.

Species **3t″** (and **3c″**) represent the direct precursors for the regioisomeric 5-*exo* and 6-*endo* pathways to follow the minimum energy path. Among the two pathways, 5-*exo* cyclization is found to be distinctly favorable energetically, as it is less expensive kinetically and is exergonic (vide infra). Commencing from **3t″**, formation of **4s** takes place through a chairlike transition state TS[**3t″**−**4s**] in which the newly formed $C^5$−N $\sigma$-bond has a distance of 2.10 Å (Figure 1). Ring closure via TS[**3t″**−**4s**] affords the five-membered azacycle that is ac-

(15) (a) Ahlrichs, R.; Bär, M.; Häser, M.; Horn, H.; Kölmel, C. *Chem. Phys. Lett.* **1989**, *162*, 165. (b) Treutler, O.; Ahlrichs, R. *J. Chem. Phys.* **1995**, *102*, 346. (c) Eichkorn, K.; Treutler, O.; Öhm, H.; Häser, M.; Ahlrichs, R. *Chem. Phys. Lett.* **1995**, *242*, 652.
(16) (a) Dirac, P. A. M. *Proc. Cambridge Philos. Soc.* **1930**, *26*, 376. (b) Slater, J. C. *Phys. Rev.* **1951**, *81*, 385. (c) Vosko, S. H.; Wilk, L.; Nussiar, M. *Can. J. Phys.* **1980**, *58*, 1200. (d) Becke, A. D. *Phys. Rev.* **1988**, *A38*, 3098. (e) Perdew, J. P. *Phys. Rev.* **1986**, *B33*, 8822; *Phys. Rev. B* **1986**, *34*, 7406.
(17) For instance, see: (a) Tobisch, S.; Nowak, Th.; Boegel, H. *J. Organomet. Chem.* **2001**, *619*, 24. (b) Heiber, H.; Gropen, O.; Laerdahl, J. K.; Swang, O.; Wahlgreen, U. *Theor. Chem. Acc.* **2003**, *110*, 118.
(18) Tobisch, S. *Chem. Eur. J.* **2005**, *11*, 3113.
(19) For further details, see: www.struked.de.
(20) For substrate adducts **X**-S, the -S(t) and -S(c) suffixes denotes the 4*E*(trans) and 4*Z*(cis) isomers of the heptadien-1-amine aminodiene substrate **1**.
(21) For protonolysis of $Cp^*_2LnCH(TMS)_2$ by amines a turnover frequency of ∼1 × 10$^7$ h$^{-1}$ (293.15 K) has been reported in ref 4b. In a crude approximation, the experimentally determined TOF corresponds to a value of about 12.5 kcal mol$^{-1}$ for $\Delta G^{\ddagger}$, thus being in good agreement to each another, by applying the Eyring equation with $k = (2.08 \times 10^{10}) \times T \times \exp(-\Delta G^{\ddagger}/RT)$.
(22) For NMR evidence of rapid amido/amine permutation and association of free amine, see ref 4b.
(23) This is supported by X-ray structural characterization of the [($\eta^5$-$C_5Me_5$)$_2$-$LaNHCH_3(H_2NCH_3)$] compound (ref 4b).

***Table 1.*** Activation Enthalpies and Free Energies and Reaction Enthalpies and Free Energies for Cyclization of **3** Occurring through the Alternative Regioisomeric 5-*exo* and 6-*endo* Pathways[a,b]

| cyclization pathway | precursor[c] | TS | product[d] |
|---|---|---|---|
| 5-*exo* **4s**-generating pathway | 1.6/*−0.1* (**3t′**)<br>0.0/*0.0* (**3t″**) | 5.7/*7.6* ($\Delta S^{\ddagger} = -6.4$ eu)[e] | −4.7/*−2.8* (**4s**) |
| 5-*exo* **4a**-generating pathway | 5.3/*2.7* (**3c′**)<br>3.7/*3.6* (**3c″**) | 8.4/*9.8* ($\Delta S^{\ddagger} = -4.7$ eu)[e] | −2.9/*−1.2* (**4a**) |
| 6-*endo* pathway | 0.0/*0.0* (**3t″**) | 41.9/*44.3* ($\Delta S^{\ddagger} = -7.9$ eu)[e] | 31.7/*33.9* (**5**) |
| | aminodiene substrate-assisted process[f] | | |
| 5-*exo* **4s**-generating pathway | −10.1/*−2.4* (**3t′**-S(t))<br>−5.5/*2.5* (**3t″**-S(t)) | 9.3/*19.0* ($\Delta S^{\ddagger} = -32.5$ eu)[e] | −8.0/*2.6* (**4s**-S(t)) |
| 6-*endo* pathway | −10.1/*−2.4* (**3t′**-S(t)) | 34.8/*44.8* ($\Delta S^{\ddagger} = -33.7$ eu)[e] | 23.5/*33.5* (**5**−S(t)) |

[a] Total barriers, reaction energies, and activation entropies are relative to **3t″** with a chairlike chelating diene functionality. [b] Activation enthalpies and free energies ($\Delta H^{\ddagger}/\Delta G^{\ddagger}$) and reaction enthalpies and free energies ($\Delta H/\Delta G$) are given in kilocalories per mole; numbers in italic type are the Gibbs free energies. [c] See the text (or Figure S1) for description of the various isomers of **3t**, **3c**. [d] See Scheme 1 for description of the azacyclic cyclization products. [e] The activation entropy is given in entropic units ≡ cal mol$^{-1}$ K$^{-1}$. [f] The process to be assisted by an additionally coordinating aminodiene molecule has been investigated with **1t** as the substrate. Total barriers, reaction energies, and activation entropies are relative to {**3t″** + **1t**}.

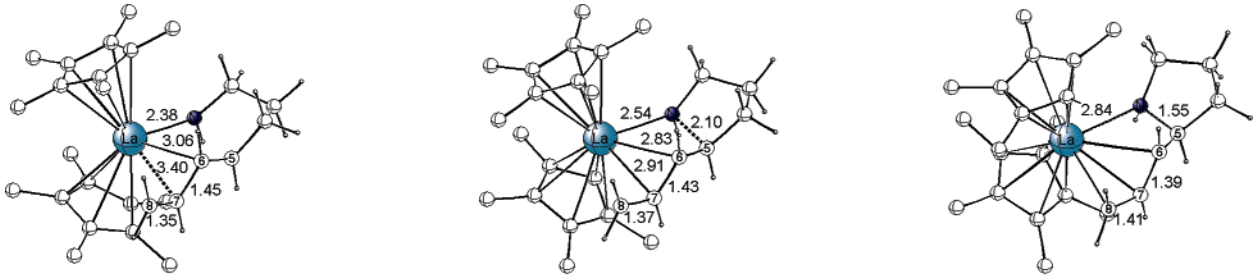


***Figure 1.*** Selected geometric parameters (angstrom) of the optimized structures of key species for the favorable 5-*exo* cyclization pathway. The cutoff for drawing La−C bonds was arbitrarily set to 3.1 Å. The hydrogen atoms on the methyl groups of the catalyst backbone are omitted for the sake of clarity.

companied by transformation of the diene moiety into a syn-$\eta^3$-butenyl functionality, both of which occur in a concerted fashion. Noteworthy, the diene's C$^7$═C$^8$ double bond, which does not participate in the C−N bond formation, assists the process actively by stabilizing the lanthanide center coordinatively. Decay of the transition state leads to **4s** as the initially formed and prevalent cyclization product, where the azacycle is coordinated by its N-donor center and also by the syn-$\eta^3$-butenyl tether group to La (Figure 1).

The **3t″** → **4s** 5-*exo* cyclization is predicted to be a kinetically feasible process, which is connected with a moderate barrier ($\Delta G^{\ddagger} = 7.6$ kcal mol$^{-1}$) and driven by a small thermodynamic force ($\Delta G^{\ddagger} = -2.8$ kcal mol$^{-1}$, Table 1), thus being likely to occur in a reversible fashion. A compact chairlike transition-state structure is encountered, which is reflected in the estimated negative activation entropy of −6.4 eu. The alternative 5-*exo* pathway that starts from **3c″** is connected with a similar energy profile (Table 1), but it is kinetically more expensive ($\Delta\Delta G^{\ddagger} =$ 2.2 kcal mol$^{-1}$) and thermodynamically less favorable ($\Delta\Delta G$ = 1.6 kcal mol$^{-1}$). Nevertheless, 5-*exo* cyclization to afford **4s** and **4a** is facile for both cases, with **3t″** → **4s** most feasible energetically. Ring closure via **3t″** → **5** to afford the six-membered azacycle, however, is predicted to be highly difficult kinetically, as it is connected with an insurmountably high barrier of 44.3 kcal mol$^{-1}$ ($\Delta G^{\ddagger}$), and is also strongly endergonic ($\Delta G$ = 33.9 kcal mol$^{-1}$, Table 1). Thus, 6-*endo* cyclization is clearly seen to be distinctly disfavored energetically relative to the 5-*exo* pathway due to both kinetic ($\Delta\Delta G^{\ddagger} = 36.7$ kcal mol$^{-1}$) and thermodynamic ($\Delta\Delta G$ = 36.7 kcal mol$^{-1}$) factors. The strong kinetic preference of 5-*exo* versus 6-*endo* cyclization has its primary origin in the coordinative assistance of the 5-*exo* pathway by the C$^7$═C$^8$ double bond, which is not effective for the 6-*endo* pathway (cf. Supporting Information).

As a further important aspect, the possible supporting influence of excess substrate **1t** has been examined. Although the precursor exists predominantly as **3t′**-S(t) adduct (cf. section I.A), added substrate does not appear to facilitate 5-*exo* cyclization either kinetically or thermodynamically. It is therefore not likely to assist in this process. As a consequence, the substrate must dissociate from the precursor prior to ring closure (see the Supporting Information for more details).

**C. Isomerization of the Allylic Tether Group of the 5-*exo* Cyclization Product.** This section addresses the question as to whether the 5-*exo* cyclization products **4s** and **4a** bearing a five-membered azacycle with a syn- or anti-$\eta^3$-butenyl−La coordinated tether group, respectively, are present in a kinetically mobile equilibrium or not. This is of critical importance for the elucidation of the stereoregulation, as the relative kinetics for generation (cf. section I.B), consumption (cf. section I.D), and mutual interconversion of **4s**, **4a**, together with their relative thermodynamic population are crucial factors that determine the distribution of the various pyrrolidines (Scheme 1).

The **4s**, **4a** isomers are found to be similar in free energy, with **4s** being slightly prevalent (Table S2). Thus, their interconversion is an essentially thermoneutral process. The favorable path to follow for this transformation entails $\eta^3$-$\pi$ → $\eta^1$(C$^6$)-$\sigma$-allylic rearrangement and encounters the $\eta^1$(C$^6$)-$\sigma$-butenyl−La rotational transition state TS$_{ISO}$[**4**].[24−26] Allylic **4s**

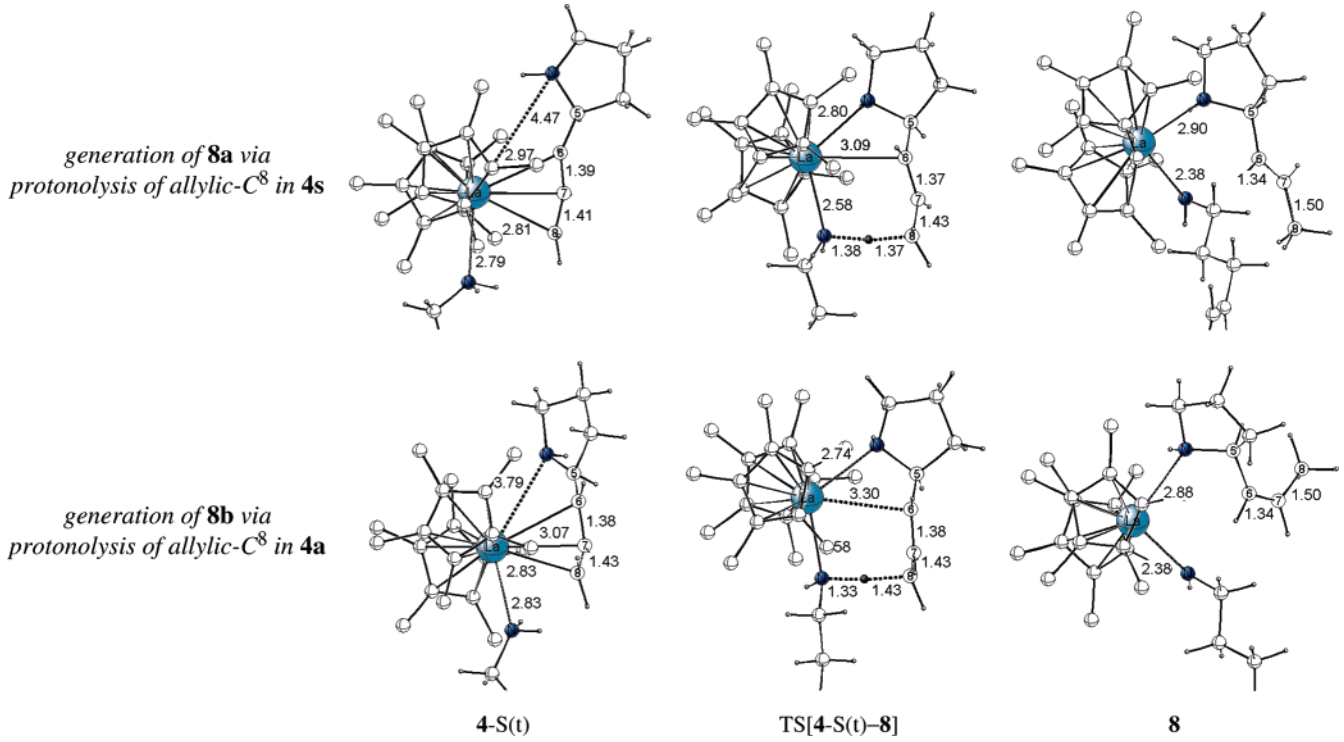


***Figure 2.*** Selected geometric parameters (angstrom) of the optimized structures of key species for the favorable pathway for protonolysis of the $\eta^3$-allyl-azacycle−La compound **4** by aminodiene substrate **1t** affording the cycloamine-amido−La species **8a**, **8b** along alternative pathways. The cutoff for drawing La−C bonds was arbitrarily set to 3.1 Å. The hydrogen atoms on the methyl groups of the catalyst backbone are omitted for the sake of clarity. Please note that the amino-/amidodiene moiety and the catalyst's backbone are displayed in a truncated fashion for several of the species.

$\rightleftarrows$ **4a** isomerization is predicted to possess a significant barrier ($\Delta G^{\ddagger}$ = 19.8 kcal mol$^{-1}$, Table S2), which is of the same magnitude as determined experimentally for related ($\eta^3$-allyl)$_3$−La complexes.[14b,d,27] This indicates this step as being kinetically difficult when compared to intramolecular cyclization and ensuing protonolysis. Excess substrate **1** is found to not facilitate the isomerization kinetically. A more detailed characterization of this step including the key species (Figure S4) and the complete energy profile (Table S2) can be found in the Supporting Information.

**D. Protonolysis of Five-Membered Azacyclic Intermediates.** After the intramolecular insertion step occurs to generate **4a**, **4s** and **5**, ensuing protonolysis by aminodiene substrate **1t** leads to the respective cycloamine-amido−La compounds, from which **3t″** is readily regenerated through a kinetically facile cycloamine product expulsion (Scheme 1). As revealed from section I.B, the thermodynamic population of **5** is likely to be negligible, owing to the kinetically precluded, strongly endergonic 6-*endo* cyclization. As a consequence, the path for protonolysis of **5**, which would afford 2-vinyl-piperidine **7**, remains entirely closed, irrespective of whether protonolysis is kinetically feasible or not. Therefore, the protonolysis that starts from **4s**, **4a** is exclusively investigated, and the discussion is primarily focused on the favorable pathways for proton transfer onto the terminal, unsubstituted butenyl-C$^8$ carbon. These pathways are structurally characterized in Figure 2 and first form cycloamine-amido−La species **8a**, **8b**, from which **6a** and **6b** are subsequently released, respectively. The regioisomeric pathways for protonation of the substituted butenyl-C$^6$ is predicted to be distinctly impeded kinetically; a detailed description is included in the Supporting Information. Table 2 collects the complete energetics.

For precursor adducts[20] **4s**-S(t), **4a**-S(t) to be formed, the substrate has to compete for coordination with the azacycle that is attached to La by its nitrogen lone pair in **4s**, **4a**. As revealed from Figure 2, this interaction almost entirely disappears upon complexation of **1t**. Substrate uptake is predicted to be a slightly exothermic process ($\Delta H$, Table S2). A transition-state structure constituting the simultaneous N−H bond cleavage and C−H bond formation is encountered along the minimum-energy path. Commencing from **4s**-S(t), **4a**-S(t) with an $\eta^3$-allylic tether group, the C$^8$ carbon to be protonated becomes displaced from the immediate proximity of the lanthanide center upon traversing through the transition state, which is furthermore characterized by a partial allyl → vinyl conversion. This reduction of the coordination sphere around the La atom is counterbalanced in TS[**4s**-S−**8a**] and TS[**4a**-S−**8b**] by a closer approaching azacyclic moiety (Figure 2).

Of the alternative **4s** + **1t** → **8a** and **4a** + **1t** → **8b** pathways, **4s** exhibits a higher propensity to undergo protonation. The first pathway has a barrier of 16.0 kcal mol$^{-1}$ ($\Delta G^{\ddagger}$), while the second one is connected with an activation free energy that is 2.5 kcal mol$^{-1}$ higher ($\Delta\Delta G^{\ddagger}$, Table 2). A large negative activation entropy ($\Delta S^{\ddagger} = -(31.0-31.6)$ eu) is associated with protonolysis. This large negative value originates predominantly from formation of the first amine-amido−La adduct. Release of the cycloamine products via **8a**/**8b** + **1t** → **3t′**-S(t)

(24) Lukas, J.; van Leeuwen, P. W. N. M.; Volger, H. C.; Kouwenhoven, A. P. *J. Organomet. Chem.* **1973**, *47*, 163.
(25) (a) Faller, J. W.; Thomsen, M. E.; Mattina, M. J. *J. Am. Chem. Soc.* **1971**, *93*, 2642. (b) Vrieze, K. Fluxional Allyl Complexes. In *Dynamic Nuclear Magnetic Resonance Spectroscopy*; Jackmann, L. M., Cotton, F. A., Eds.; Academic Press: New York, 1975.
(26) Tobisch, S.; Taube, R. *Organometallics* **1999**, *18*, 3045.

***Table 2.*** Activation Enthalpies and Free Energies and Reaction Enthalpies and Free Energies for Protonolysis of the $\eta^3$-Allyl−La Intermediate **4** by Amidodiene Substrate **1t** to Afford the Cycloamine-Amido−La Compounds **8a**−**8c** along Various Regioisomeric Pathways for Proton Transfer[a,b]

| | cycloamine-generating pathway | | |
|---|---|---|---|
| cyclization pathway | **4**-S(t)[c] | TS | **8**[c] |
| 5-*exo* pathway | | | |
| **8a**/**6a** via H-trf onto $C^8$ of **4s** | 1.9/*10.3* (**4s**-S(t))[d] | 6.6/*16.0* ($\Delta S^{\ddagger} = -31.6$ eu)[e] | 2-[(*E*)-prop-1-enyl]pyrrolidine −5.2/*2.2* (**8a**) |
| **8b**/**6b** via H-trf onto $C^8$ of **4a** | 3.1/*11.8* (**4a**-S(t))[d] | 9.3/*18.5* ($\Delta S^{\ddagger} = -31.0$ eu)[e] | 2-[(*Z*)-prop-1-enyl]pyrrolidine −3.6/*4.0* (**8b**) |
| **8c**/**6c** via H-trf onto $C^6$ of **4s**/**4a** | −3.3/*5.4* (**4s**-S(t)) | 14.0/*22.3* ($\Delta S^{\ddagger} = -27.7$ eu)[e] | 2-(prop-2-enyl)pyrrolidine −0.6/*7.4* (**8c**) |

| | substrate-assisted cycloamine-generating pathway[f] |
|---|---|
| cyclization pathway | TS |
| 5-*exo* pathway[g] | |
| **8a**/**6a** via H-trf onto $C^8$ of **4s** | 13.6/*30.6* ($\Delta S^{\ddagger} = -56.9$ eu)[e] |
| **8b**/**6b** via H-trf onto $C^8$ of **4a** | 11.2/*28.4* ($\Delta S^{\ddagger} = -57.5$ eu)[e] |
| 5-*exo* pathway[h] | |
| **8a**/**6a** via H-trf onto $C^8$ of **4s** | 17.9/*34.5* ($\Delta S^{\ddagger} = -55.8$ eu)[e] |
| **8b**/**6b** via H-trf onto $C^8$ of **4a** | 15.8/*32.3* ($\Delta S^{\ddagger} = -55.2$ eu)[e] |

[a] Total barriers, reaction energies, and activation entropies are relative to {**4s** + **1t**}. [b] Activation enthalpies and free energies ($\Delta H^{\ddagger}/\Delta G^{\ddagger}$) and reaction enthalpies and free energies ($\Delta H/\Delta G$) are given in kilocalories per mole; numbers in italic type are the Gibbs free energies. [c] See the text (or Figure 2, S5) for description of the various isomers of the amine adducts **4**-S and of the cycloamine-amido product complex **8**. [d] The precursor species for the **8a**/**6a**- and **8b**/**6b**-generating pathways are not identical with the most stable **4s**/**4a**-S(t) adduct species reported in Table S2. [e] The activation entropy is given in entropic units ≡ cal mol$^{-1}$ K$^{-1}$. [f] The process to be assisted by an additive aminodiene molecule has been investigated with methylamine ($MeNH_2$, S′) as the substrate. Total barriers and activation entropies are relative to {**4s** + **1t** + $MeNH_2$}. [g] The additive substrate acts as a La-coordinated spectator ligand (Figure S6, top). [h] The additive substrate acts as a "proton shuttle" (Figure S6, bottom).

+ **6a**/**6b** is likely to be a facile,[22,28] exergonic process ($\Delta G$ = −6.2/−6.4 kcal mol$^{-1}$). The overall **1t** → **6a** transformation is exergonic, driven by a thermodynamic force of −6.3/−4.6 kcal mol$^{-1}$ ($\Delta H/\Delta G$).

Additional substrate molecules can participate in different fashions in the protonolysis step: first, as spectator ligands coordinated to La, thereby acting primarily as a counterbalance for the reduction of the coordination sphere around the lanthanide center, or second, to be directly involved in the protonolysis as a mediator for proton transfer. For **4s**/**4a** + **1t** → **8a**/**b** both alternatives have been explicitly probed computationally by the location of the transition states TS[**4**-S−**8**]-S′ and TS[**4**-S-S′−**8**], respectively, with an associated methylamine as model substrate S′ (Figure S6). For protonolysis with a directly participating substrate molecule, to traverse through TS[**4**-S-S′−**8**], the proton is transferred onto the $C^8$ carbon from an external quaternary substrate nitrogen center, which is generated by deprotonation of the terminal ammonium group of the La-coordinated aminodiene (Figure S6, bottom). Thus, the additive substrate acts as a "proton shuttle".[29] Additional substrate, either as spectator or as moderator, does not act to stabilize the transition states for the two favorable protonolysis pathways, on either the $\Delta H$ or the $\Delta G$ surfaces (Table 2). Thus, the additional amine does not appear to serve to accelerate these pathways kinetically. This leads us to the conclusion that excess substrate is not likely to assist the protonolysis of azacycle−La intermediates **4s**, **4a**, which can reasonably be extended to the precatalyst activation step (cf. section I.A).

**II. Catalytic Reaction Course of Aminodiene IHC. A. Free-Energy Profiles.** The condensed free-energy profile, comprising solely of viable pathways for crucial elementary steps of the tentative catalytic cycle (Scheme 1) is presented in Scheme 2. More detailed energy profiles are included in the Supporting Information. Having this profile in our hands, together with the critical exploration of crucial elementary steps undertaken in previous sections, allows us to draw the following conclusions. (1) Among compounds **3t′**-S, **4s**, and **8a**, which are predicted to be the thermodynamically prevalent species occurring within the catalytic reaction course, **3t′**-S is the most likely candidate to be the catalyst's resting state under actual reaction conditions.[8d,30] This is consistent with the many experimental data that show the amine-amido−Ln species **3t′**-S to be the resting state.[4b,7,8] (2) For intramolecular cyclization to occur along the favorable 5-*exo* pathway, the substrate first must dissociate or become displaced from **3t′**-S (cf. section I.B). This conforms with experimental data for octadienylamine cyclization,[8b] arguing for the first substrate displacement from the resting state species. (3) Protonolysis of **4s**, **4a** by **1t** is also indicated to not be assisted by additive substrate molecules. (4) Intramolecular 5-*exo* cyclization via **3t″**/**3c″** → **4s**/**4a** and ensuing protonolysis along **4s**/**4a** + **1t** → **8a**/**8b** are the crucial steps that determine the activity and selectivity of the overall cycloamination reaction. Alternative pathways for these steps as well as **4s** ⇄ **4a** allylic isomerization are found to be more difficult kinetically. Hence, they are not accessible under catalytic reaction conditions. (5) Cyclization is predicted to be a slightly exergonic step ($\Delta G$ = −2.8 kcal mol$^{-1}$) that has only a moderate barrier ($\Delta G^{\ddagger}$ = 7.6 kcal mol$^{-1}$), thus likely being a facile and reversible process.

(27) The free-energy barrier for allylic isomerization has been determined by NMR to ∼16.0 kcal mol$^{-1}$ for [($\eta^5$-Cp′)La($\eta^3$-$C_3H_5)_3$]$^-$ (Cp′ = $C_5H_5$, $C_5Me_5$, $C_9H_7$, $C_{13}H_9$) complexes (ref 14b) and to >15.5 kcal mol$^{-1}$ for the [La($\eta^3$-$C_3H_5)_3$] dioxane adduct (ref 14d).

(28) The examination by a linear transit approach revealed no indication that this process is connected with a significant enthalpic barrier.

(29) Senn, H. M.; Blöchl, P. E.; Togni, A. *J. Am. Chem. Soc.* **2000**, *122*, 4098.

(30) Please note that the condensed free-energy profile is computed for standard conditions (298.15 K, 1 atm, stoichiometric amount of aminodiene substrate). The large substrate excess, however, favors the generation of adducts, like **3t′**-S(t). The correction of **3t″** + S(t) → **3t′**-S(t) adduct formation for concentration effects according to $\Delta G = \Delta G^{\circ} - RT \times \ln([\mathbf{3t'}\text{-S(t)}] \times [\mathbf{3t''}]^{-1} \times [\text{S(t)}]^{-1})$ reduces the free energy by $RT \times \ln([\text{S(t)}]^{-1})$, which amounts to 2.6 kcal mol$^{-1}$ by considering real reaction conditions (80 molar excess of S(t), 298.15 K, 1 atm).

***Scheme 2.*** Condensed Gibbs Free-Energy Profile of the Intramolecular Hydroamination/Cyclization of (4*E*/*Z*,6)-Heptadien-1-amine **1t**, **1c** Mediated by the $Cp^*_2LaCH(TMS)_2$ Precatalyst[a–c]

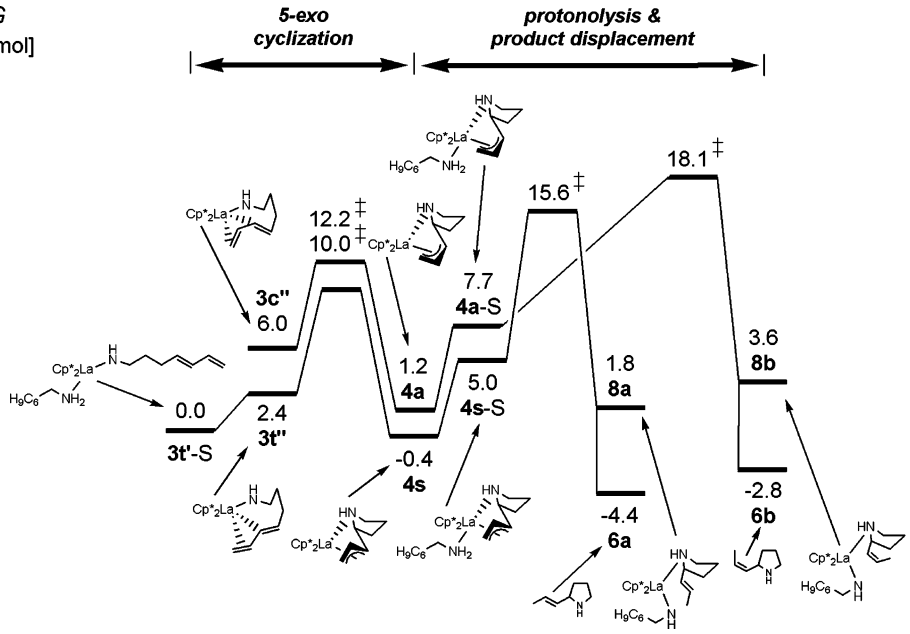


[a] Only the most feasible pathways for individual processes are included, while alternative, but unfavorable, pathways are omitted for the sake of clarity. [b] Cycloamine displacement through **8a**/**8b** + **1t** → **3t′**-S(t) + **6a**/**6b** is included. [c] See also Scheme S2, Supporting Information.

***Scheme 3.*** Proposed Mechanistic Scenario for the Organolanthanide-Mediated Intramolecular Hydroamination/Cyclization of Aminodienes

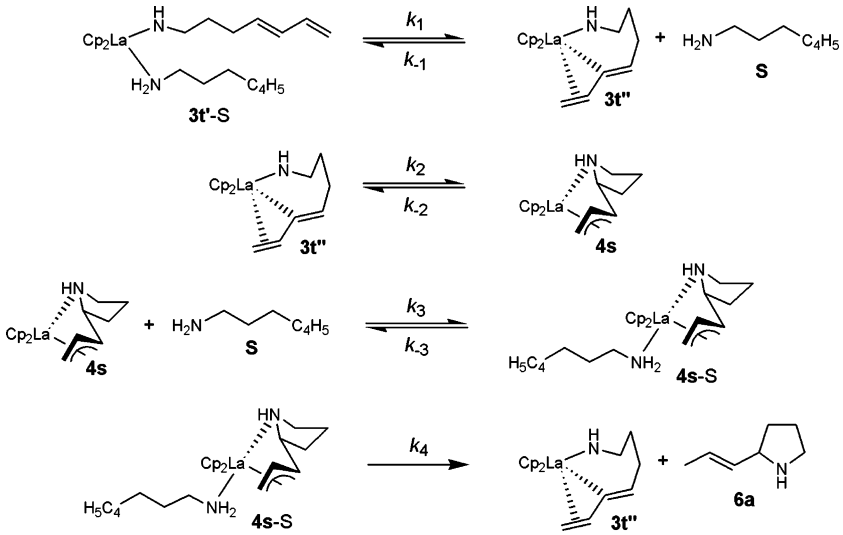


(6) Protonation has the highest kinetic barrier. This turnover-limiting protonolysis is followed by highly facile, hence almost instantaneous, **8a**/**8b** + **1t** → **3t′**-S(t) + **6a**/**6b** product displacement,[22,28] which forces the overall step downhill ($\Delta G = -4.0$ kcal mol$^{-1}$). (7) Distinctly different total free-energy barriers (i.e., relative to **3t′**-S)[31] are predicted for the most feasible pathways for unimolecular C−N bond formation and bimolecular proton transfer, with the latter kinetically significantly more expensive ($\Delta\Delta G^{\ddagger} = 5.6$ kcal mol$^{-1}$). Although the energetics of processes of different molecularity cannot be unambiguously compared at the $\Delta G$ surface, due to the employed computational methodology (cf. Supporting Information), the predicted large kinetic gap provides some confidence that protonolysis is turnover-limiting. This is corroborated further by the following kinetic analysis.

On the basis of the conclusions drawn thus far, we suggest the mechanistic scenario shown in Scheme 3 for the organolanthanide-mediated IHC of aminodienes. This scenario involves kinetically mobile, reversible aminodiene substrate dissociation/association in **3t′**-S and **4s**, facile C=C insertion into the La−N bond and turnover-limiting protonolysis ($k_4 \equiv k_{prod}$). Commencing from the resting state **3t′**-S, the substrate must first dissociate for 5-*exo* cyclization to proceed, readily giving rise to **3t″** with a chelating diene functionality. Ensuing facile **3t″** → **4s** cyclization through a compact chairlike transition-state structure is connected with a negative activation ($\Delta S^{\ddagger} = -4.6$ eu) and reaction entropy ($\Delta S = -4.6$ eu). Generation of pyrrolidine products takes place via first rapid substrate association to the cyclization product and subsequent protonolysis of the $\eta^3$-butenyl−La bond by aminodiene substrate. The entropic contributions for substrate association/dissociation

(31) Total enthalpies ($\Delta H_{tot}$), free energies ($\Delta G_{tot}$), and entropies ($\Delta S_{tot}$) are given relative to the catalyst's resting state **3t′**-S, corrected by the respective number of substrate molecules.

equilibria $K_1$ ($\Delta S = 26.2$ eu), $K_3$ ($\Delta S = -29.2$ eu) essentially compensate each other. The proton-transfer step is linked to the highest absolute free-energy barrier of all relevant steps and is characterized by a negative $\Delta S^{\ddagger}$ of $-2.4$ eu relative to **4s**-S. Kinetic analysis assuming rapid equilibria $K_1$, $K_3$ and applying steady-state concentrations[32a] for **4s**[32b] yields the rate law of eq 2, which predicts first-order behavior in [catalyst].[33]

$$\text{velocity} = k_4 K_1 k_2 k_{-3} \times [\mathbf{3t'}\text{-S}] \times [\text{S}]^{-1} \qquad (2)$$

Although aminodiene substrate participates in the turnover-limiting step, the kinetics is nevertheless zero-order in [substrate] due to associated $K_1$, $K_3$ equilibria. For this mechanistic scenario, an effective total activation barrier of 14.6 kcal mol$^{-1}$ ($\Delta H_{tot}^{\ddagger}$)[31] is predicted for protonolysis along the most feasible **8a**-generating pathway (cf. Supporting Information),[34] which agrees very well with the experimentally determined enthalpic barrier for the turnover-limiting step.[8d] A negative total activation entropy ($\Delta S_{tot}^{\ddagger} = -12.1$ eu)[31] is associated with proton transfer, which originates primarily from the reaction entropy for cyclization and the intrinsic activation entropy for protonation (vide supra); thus giving rise to an effective activation free energy of 18.2 kcal mol$^{-1}$ ($\Delta G_{tot}^{\ddagger}$).[31] The mechanistic scenario suggested here together with the computed energy profile is consistent with the empirical rate law (eq 1) and accounts for crucial experimental observations.[8] It furthermore allows a first understanding of the origin of the measured negative $\Delta S^{\ddagger}$, although the computationally estimated activation is substantially smaller than the measured value.[8d] This discrepancy may arise because of the employed computational methodology. It has been observed by NMR that variable numbers of amine molecules are coordinated to the lanthanide center. Furthermore, a facile exchange process rapidly permutes not only lanthanide amido and coordinated amine but also coordinated and free amine.[4b,7] Therefore, a variable number of spectator substrate molecules are presumably involved in $K_1$, $K_3$ equilibria and also in protonolysis. This, however, is accounted for herein an approximate fashion by treating a single Ln-associated substrate molecule explicitly.[35] To elaborate this aspect further, molecular dynamics studies, which consider an ensemble of substrate molecules, are underway in our laboratory.

In the general mechanism proposed by Marks[7] (cf. Introduction) 5-*exo* cyclization is assumed to be turnover-limiting (i.e., $k_2 \equiv k_{prod}$ in Scheme 3). This scenario gives rise to a rate law[36] that predicts first- and zero-order dependence in [catalyst] and [substrate], respectively. This law is as consistent with the empirical law (eq 1) as eq 2 is. However, as revealed from Schemes S1, S2,[31,34] the ring closure is connected with a large positive $\Delta S_{tot}^{\ddagger}$ of 26.2 eu, due to the $K_1$ equilibrium. This is in sharp contrast to experimental observations,[8] hence ruling this mechanistic scenario out for aminodiene cycloamination.

As already mentioned at the outset, the recent computational study[12] by Marks and co-worker predicted intramolecular cyclization to be the rate-determining step in IHC of aminoalkenes. For this substrate as well, the amine-amido−Ln species (i.e., the congener of **3t′**-S) is likely to be the catalyst's resting state, which is consistent with experiments.[4b,7] Provided that the aminoalkene must dissociate from the amine-amido−Ln compound prior to C−N bond formation, which is supported by experimental data,[4b] then a large positive $\Delta S_{tot}^{\ddagger}$ should be associated with the rate-controlling step. Hence, the origin of the measured large negative $\Delta S^{\ddagger}$ is not understood thus far for aminoalkene cycloamination, and further detailed computational studies are necessary.

**B. Factors Governing the Regioselectivity and Double Bond Selectivity.** The intramolecular insertion of the C═C diene functionality into the La−N bond in **3** is seen to be the crucial step that determines whether cycloamines with a five- or six-membered ring are formed. The 5-*exo* pathway is predicted to be distinctly favorable over the alternative 6-*endo* pathway by both thermodynamic and kinetic factors. This has its primary origin in the coordinative assistance of the 5-*exo* pathway by the C$^7$═C$^8$ diene double bond, which is not effective for the latter (cf. section I.B). The computed kinetic gap of 36.7 kcal mol$^{-1}$ ($\Delta\Delta G^{\ddagger}$, Table 1) between the alternative pathways that start from precursor **3t″** clearly reveals the intramolecular cyclization to proceed with almost complete regioselectivity, to form the five-membered azacycle exclusively. This is consistent with the experimental observation that piperidines are not among the reaction products.

Precursor species **4a**, **4s** for protonolysis are not present in equilibrium, as allylic isomerization is seen to be kinetically disabled due to a significant barrier ($\Delta G^{\ddagger} = 19.8$ kcal mol$^{-1}$). This indicates the **4s** ⇄ **4a** conversion to be distinctly slower than ensuing protonolysis following the most feasible pathways. Cyclization via **3t″** → **4s** and **3c″** → **4a** is facile. The first is kinetically more favorable ($\Delta\Delta G^{\ddagger} = 2.2$ kcal mol$^{-1}$), so that both **4s** and **4a** are present, but in different concentrations. Consequently, the distribution of the pyrrolidine products **6a**−**6c** is regulated by both thermodynamic and kinetic factors: (1) by the thermodynamic populations of **4s**, **4a**, which are determined by the relative proportions of the substrate isomers (1:440 for 4*Z*/4*E*-isomers, cf. Supporting Information) as well as by the rate for **3t″**/**3c″** → **4s**/**4a** cyclization and (2) by their propensity to undergo protonolysis following the various competing pathways.

Of the alternative pathways for proton transfer onto the reactive C$^6$ and C$^8$ centers of the allylic tether in **4**, the latter is predicted to be distinctively preferred both kinetically and thermodynamically, as it benefits from coordinative stabilization by the azacyclic moiety. The predicted kinetic gap of 6.3 kcal mol$^{-1}$ ($\Delta\Delta G^{\ddagger}$, Table 2) for **4s** + **1t** → **8a**/**8c** → **6a**/**6c** can be regarded as being large enough to suppress the formation of **6c** almost entirely. Accordingly, protonolysis of **4** occurs in a highly regioselective fashion, which rationalizes the exclusive formation of 2-(prop-1-enyl)pyrrolidines **6a**, **6b**.[8b,d] With regard to the double bond selectivity, (1) **4s** is present in higher concentrations than **4a** (vide supra) and (2) the **4s** + **1t** → **8a** → **6a** pathway is predicted to be kinetically easiest ($\Delta\Delta G^{\ddagger} = 2.5$ kcal mol$^{-1}$

(32) (a) Espenson, J. H. *Chemical Kinetics and Reaction Mechanisms*, 2nd ed.; McGraw-Hill: New York, 1995. (b) Compound **4s** is likely to be a transient species, thus being present in negligible stationary concentrations, because its formation via reversible **3t″** → **4s** cyclization and ensuing **4s** + S(t) → **4s**-S(t) substrate association are facile processes.

(33) The rate law (eq 2) does also account for substrate self-inhibition effects that have been experimentally observed in octadienylamine cycloamination (ref 8b)

(34) See Scheme S1 and S2, respectively, by taking the actual reaction conditions into account (ref 30).

(35) It should be noted that the prediction of accurate entropies for lanthanide- as well as for transition-metal-assisted processes taking place in condensed phase remains still a frontier in computational chemistry.

(36) Under similar assumptions as those for eq 2, one obtains: velocity = $k_2 K_1 \times [\mathbf{3t'}\text{-S}] \times [\text{S}]^{-1}$.

between **8a**/**8b**-generating pathways), thereby implying that **6a** is the cycloamine that is predominantly formed. This result conforms with the experimentally observed 84:16 ratio of *E*/*Z*-isomers of 2-(prop-1-enyl)pyrrolidine.[8b,d]

## Concluding Remarks

We have presented, to the best of our knowledge, the first detailed computational mechanistic exploration of the complete catalytic reaction course for the organolanthanide-mediated intramolecular hydroamination/cyclization (IHC) of conjugated aminodienes with a prototypical achiral lanthanocene-based catalyst by means of a reliable gradient-corrected DFT method. The following objectives have been achieved: (1) All crucial elementary steps for a tentative catalytic cycle (Scheme 1) have been thoroughly characterized in terms of structural and energetic aspects. (2) A mechanistic scenario has been proposed based on a comprehensive computational study (Scheme 3) that (a) is consistent with the determined empirical rate law, (b) revealed the identity of the turnover-limiting step, and (c) provided a first understanding of the origin of the measured negative $\Delta S^{\ddagger}$. With substrate adduct **3t′**-S as the catalyst's resting state, this scenario involves rapid equilibria of substrate association/dissociation and facile intramolecular diene insertion, followed by a turnover-limiting protonolysis of the $\eta^3$-butenyl−Ln functionality. The computed effective kinetics ($\Delta H_{tot}^{\ddagger} = 14.6$ kcal mol$^{-1}$, $\Delta S_{tot}^{\ddagger} = -12.1$ eu) are in reasonably good agreement with experimental data. This mechanistic scenario revises the general proposal by Marks[7] for the organolanthanide-assisted cycloamination of aminodienes. Whether this mechanism can be generalized to IHC of other unsaturated C−C functionalities will be the subject of forthcoming investigations. (3) The thermodynamic and kinetic factors that determine the high regio- and stereoselectivity have been elucidated.

**Acknowledgment.** I wish to thank Professor Tom Ziegler (University of Calgary, Canada) for his generous support. I would also like to thank one of the Referees for the valuable suggestions to improve the manuscript. Excellent service by the computer centers URZ Halle and URZ Magdeburg is gratefully acknowledged.

**Supporting Information Available:** Full descriptions of the geometry of all reported key species (Cartesian coordinates in angstroms). Complete characterization of crucial elementary steps (Figures S1−S6, Tables S1, S2), computational details, and validation of the employed computational method (Tables S3−S5) are included (PDF). This material is available free of charge via the Internet at http://pubs.acs.org.

JA042546H